

MAVEN observation study of the effects of crustal magnetic fields on the ratio of N_e/N_{CO_2} of Martian ionosphere

Zhou Chen^{1,2}, Jinsong Wang³, Haimeng Li^{1,2}, Shiyong Huang⁴, Xiaohua Deng^{1,2}, Sheng Hong²

¹Institute of Space Science and Technology, Nanchang University, Nanchang, China

²Information Engineering School, Nanchang University, Nanchang, China

³Key Laboratory of Space Weather, National Center for Space Weather, Meteorological Administration, Beijing, China

⁴School of Electronic Information, Wuhan University, Wuhan, China

Correspondence to: Haimeng Li, lihaimeng@ncu.edu.cn

Abstract

As there are strong crustal magnetic fields in some Martian concentrated regions. it has long been a goal of Martian science to understand how crustal magnetic field affects surrounding space environment. In the paper, using the data measured by MAVEN, the ratio of electron/ CO_2 density (N_e/N_{CO_2}) in region with different levels of Martian ionospheric magnetic fields are studied. It seems that ratio of dayside N_e/N_{CO_2} in region with stronger ionospheric magnetic field is larger while the altitude is more than 260 km. On the other hand, the effect of crustal magnetic field intensity on the nightside ratio of N_e/N_{CO_2} is weak. Since the topological structure of magnetic field is very vulnerable to the solar wind, the correlation between N_e/N_{CO_2} and solar wind parameters are analyzed. We find that there is obvious negative correlation between dayside ratio of N_e/N_{CO_2} and solar wind dynamic pressure in the region with strong ionospheric magnetic field, which may imply that the ionospheric plasmas are significantly escaped in response to enhanced solar wind dynamic pressure pulses in the dayside region. However, the effect of solar wind on nightside ratio of N_e/N_{CO_2} is very little. These results can be useful for understanding the dynamic process in the Martian ionosphere.

Introduction

Different from earth, Mars doesn't own a global intrinsic magnetic field, but there are strong crustal magnetic fields in some concentrated regions. The area with strongest magnetic field is located at southern latitudes with longitudinal $\sim 140^\circ E - 240^\circ E$, and the magnitudes can be up to several hundred nanotesla (nT) at altitudinal ~ 400 km [Brain et al., 2003; Connerney et al., 2001]. The science question of how Martian crustal magnetic field affects surrounding space

environment is an important topic for the research of planetary science [Withers et al., 2009], it can contribute to understand the interactive behavior of Martian atmosphere-ionosphere-solar wind system. The variation of Martian magnetic field is also important to the escape rate of atmosphere [Sakai et al., 2018; Hara et al., 2018]. Moreover, Mars offers a unique laboratory for the effect of magnetic field variation on ionosphere. Previous works have suggested that Martian crustal magnetic fields have important effects on the structure of the Martian ionosphere [e.g., Gurnett et al., 2008; Withers et al., 2005]. The existence of strong crustal magnetic fields can influence the ionospheric electron density on regional scales. Andrews et al. (2015) compare electron densities above 300 km on the dayside measured by Mars Express with an revised empirical model of the Martian ionosphere (N11 model), it suggests that the magnetic field orientation and topology can influence the local electron density, and the measured values obviously exceed the value calculated from model in region with strongest crustal fields. Since the NASA’s Mars Atmospheric and Volatile Evolution (MAVEN) mission reached Martian orbit in September 2014, it provides a good opportunity to study the effects of crustal magnetic fields on the Martian ionosphere and the interaction between solar wind and ionosphere. Using MAVEN data, previous studies show that electron density in the region with stronger crustal magnetic field is higher than that with weaker crustal magnetic field (Edberg et al., 2008; Andrews et al., 2015). Flynn et al. (2017) suggests that the strong crustal magnetic fields can effectively cooling electron temperatures and enhance electron densities, because the strong closed magnetic field lines can protect ionospheric particles from erosion of solar wind, which lead to longer ionospheric plasma lifetimes, higher densities, and lower temperatures.

However, the ionospheric plasmas are mainly produced by EUV photoionization of CO_2 (Frahm et al., 2006), and the densities of CO_2 obviously vary in different regions (Barnes et al., 2017). Thus, it may be not totally precise to estimate the contribution of magnetic field to local electron density (N_e) with local CO_2 density (N_{CO_2}) neglected. The goal of this study is to reanalyze the influence of crustal field on electron density considering local CO_2 density. Using the data of electron and CO_2 densities provided by MAVEN, we calculate the ratio of electron/ CO_2 density, (N_e/N_{CO_2}), in regions with different magnetic field intensity, and analyze the effect of solar wind on N_e/N_{CO_2} in Martian ionosphere.

This paper is organized as follows: section 2 introduces the data used in this study; section 3 analyzes the effects of strong crustal magnetic field on electron density and temperature; section 4 exhibits the correlation between several solar wind parameters and ionospheric magnetic field (and N_e/N_{CO_2}), and section 5 presents discussions and conclusions.

Data set

All data used in this study are measured by MAVEN. The perigee (apogee) of MAVEN is about 150 km (~6000 km). A series of “deep-dip” campaigns can

bring the periapsis down to near 125 km. MAVEN provides detailed parameters of ionosphere, planetary corona and solar wind. Density of CO_2 is measured by Neutral Gas and Ion Mass Spectrometer (NGIMS) onboard MAVEN [Mahaffy et al., 2014] and density of electron is measured by Langmuir Probe and Waves (LPW) onboard MAVEN with time resolution of 4s [Andersson et al., 2015]. The Solar Wind Ion Analyzer (SWIA) is a part of the Particles and Fields (P & F) Package and measures the solar wind proton flow around Mars [Halekas et al., 2015]. The Magnetometer (MAG) onboard MAVEN measures the magnetic field with 32 vector samples per second [Connerney et al., 2015a, 2015b]. In this study, the magnetic field data with 1 Hz in Mars-centered Solar Orbital (MSO) coordinates are used, where +X points sunward, +Z is perpendicular to Mars orbital plane, and +Y is orthogonal to +Z and +X.

3 The ratio of electron/ CO_2 associated with magnetic field

3.1 Overview

Using the data from 2014 October 11 to 2020 March 14, we analyze both the averaged N_e/N_{CO_2} and the amplitude of magnetic field as functions of latitude and longitude. The data of magnetic field intensity and N_e/N_{CO_2} at altitude from 120 km to 400 km are divided into 30×30 grids (the size of each grid is latitudinal 6° and longitudinal 12°) on the global Martian map. Then, the averaged values (including the ratio of N_e/N_{CO_2} and magnetic field) in each grid are calculated. Figure 1a exhibits the averaged magnetic field map, which corresponds to the mean value of samples from altitudinal 120 to 400 km. It is worth noting that the maps are irrelevant to local time (LT). The averaged ratio of N_e/N_{CO_2} maps from altitudinal 300 to 400 km, 200 to 300 km, 120 to 200 km are presented in Figure 1b-d, respectively. Here the red bold lines in all maps of Figure 1 roughly denote the region with strong magnetic field intensity (>40 nT). As indicated by the red bold lines in Figure 1b and 1c, the ratio of N_e/N_{CO_2} is higher in the region with stronger ionospheric magnetic intensity. It implies that N_e/N_{CO_2} from altitudinal 200 to 400 km are strong coupled with the local magnetic field intensity. On the other hand, as shown in Figure 1d, it seems that the ratio of N_e/N_{CO_2} below 200 km is hardly related to the local magnetic field intensity.

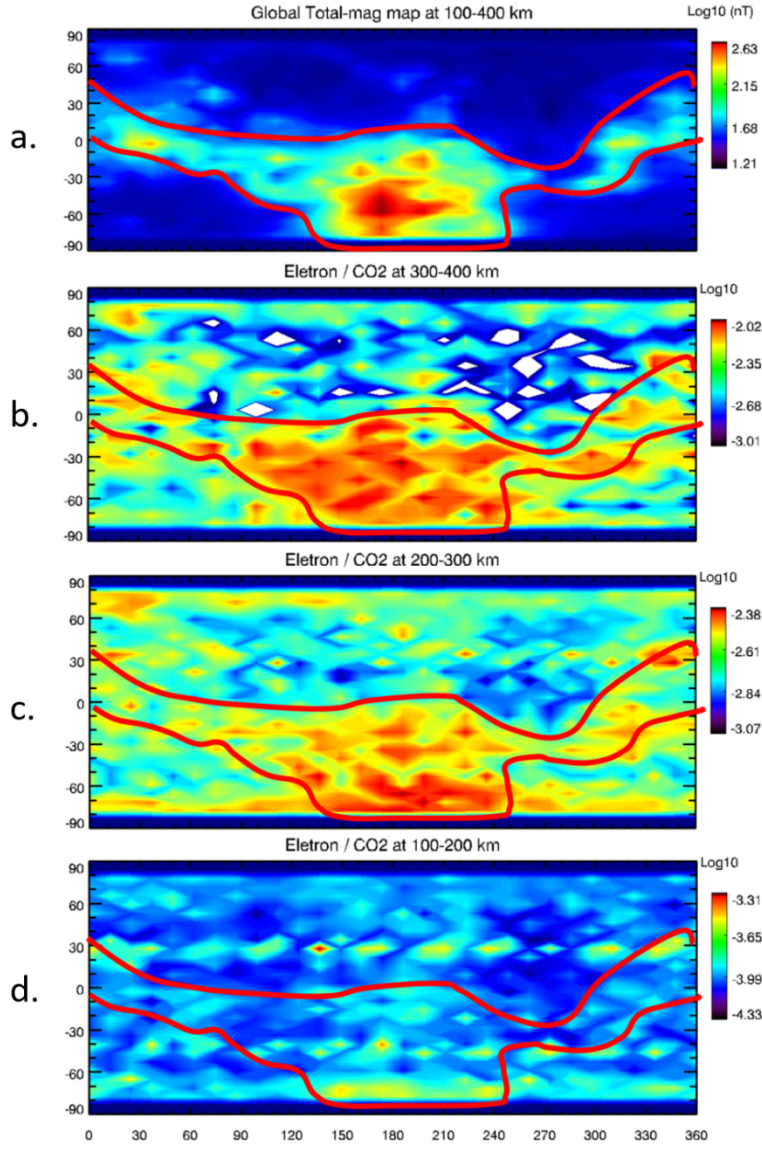


Figure 1. (a) The averaged magnetic field map, which corresponds to the mean value of samples from altitudinal 100 to 400 km, and N_e/N_{CO_2} from altitudinal (b) 300 to 400 km, (c) 200 to 300 km and (d) 120 to 200 km, respectively. The red bold lines roughly denote the region with strong magnetic field intensity (>40 nT).

In order to further quantitatively analyze the effect of crustal magnetic field on the ratio of N_e/N_{CO_2} in different ionospheric altitude, the correlations co-

efficient (CC) between ratio of N_e/N_{CO_2} and ionospheric magnetic field (from 150 to 350 km, with resolution of 5 km) are calculated and exhibited in Figure 2. As shown in Figure 2, the CC basically enhance with the increase of height, it implies that the ratio of N_e/N_{CO_2} is more obviously contributed by the intensity of magnetic field while the altitude is more than 250 km. The CC is more than 0.55 while the altitude is more than 250 km. In addition, there are two extreme values at altitudes of 310 km (CC=0.585) and 280 km (CC= 0.579), respectively.

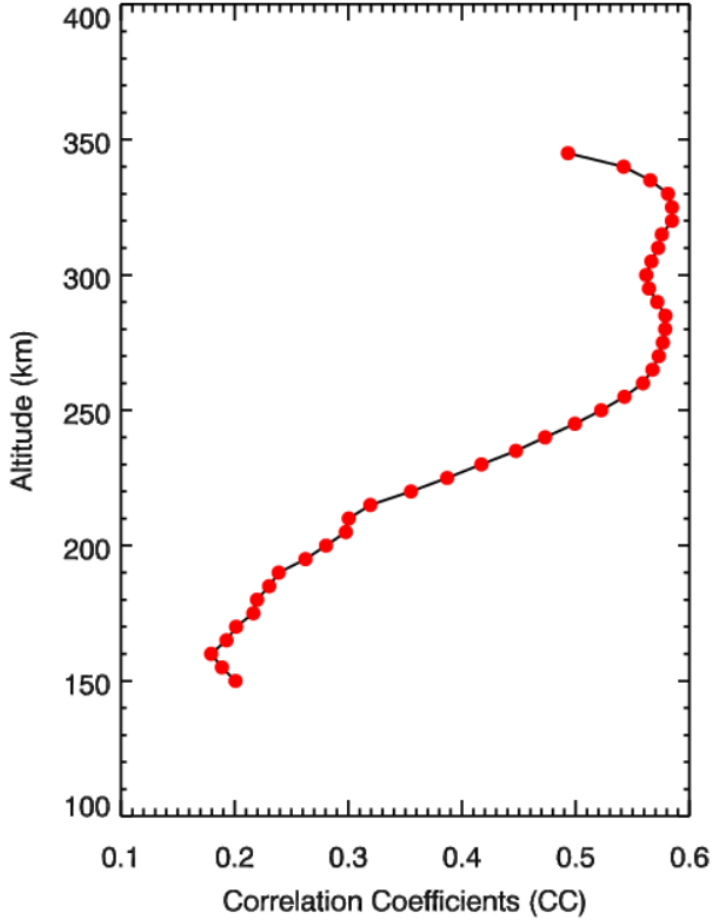


Figure 2. The Correlation between the ratio of N_e/N_{CO_2} and ionospheric magnetic field intensity as a function of altitude. **3.2 The ratios in regions with different magnetic field intensity**

The ratio of N_e/N_{CO_2} as a function of altitude in regions with different levels of magnetic field are explored. In the study, three classes of regions with different total magnetic field intensity are selected, named as regions with weak, median,

and strong magnetic field, respectively. The weak areas are the 30 grids most closed to minima value in Martian map of magnetic field intensity (less than 18 nT); the median areas are the 30 grids most closed to the median value in Martian map of magnetic field intensity (more than 25 nT, and less than 27 nT); the strong areas are the 30 grids most closed to maxima value (more than 156 nT, and less than 422 nT) in Martian map of magnetic field intensity. The averaged ratio of N_e/N_{CO_2} on both the dayside (while the solar zenith angle (SZA) of MAVEN is less than 90°) and nightside (while the SZA of MAVEN is greater than 115°) as a function of altitude (from 120 to 350 km) in the three classes of regions are shown in Figure 3. The orange lines mean the averaged dayside ratio of N_e/N_{CO_2} in region with different level of magnetic field intensity. It seems that there is more obvious positive correlation between magnetic field intensity and ratio of N_e/N_{CO_2} on the dayside than that on the nightside. As shown in the top panels of Figure 3, although the dayside ratios are similar in the three classes of regions while altitude below 200 km, it is obvious that the ratios are depend strongly on the intensity of magnetic field while the altitude is above 230 km. The mean value of the ratio in the region with strong ionospheric magnetic field is twice as much as that in region with weak ionospheric magnetic field while altitude is above 270 km. And the ratio obviously increases with the enhancement of altitude in strong and median magnetic field region (except the part near the extremum at 230 km). However, in the region with weak ionospheric magnetic field, the rate merely changes above 250 km.

As shown in the bottom panels of Figure 3. The ratio of N_e/N_{CO_2} is very low in the nightside. It seems that the correlation between nightside ratio of N_e/N_{CO_2} and ionospheric magnetic field is very weak. The profiles of ratios in three classes of regions are similar, and all the ratios in the three classes are very low, although the ratios increase with enhancement of altitude below 230 km.

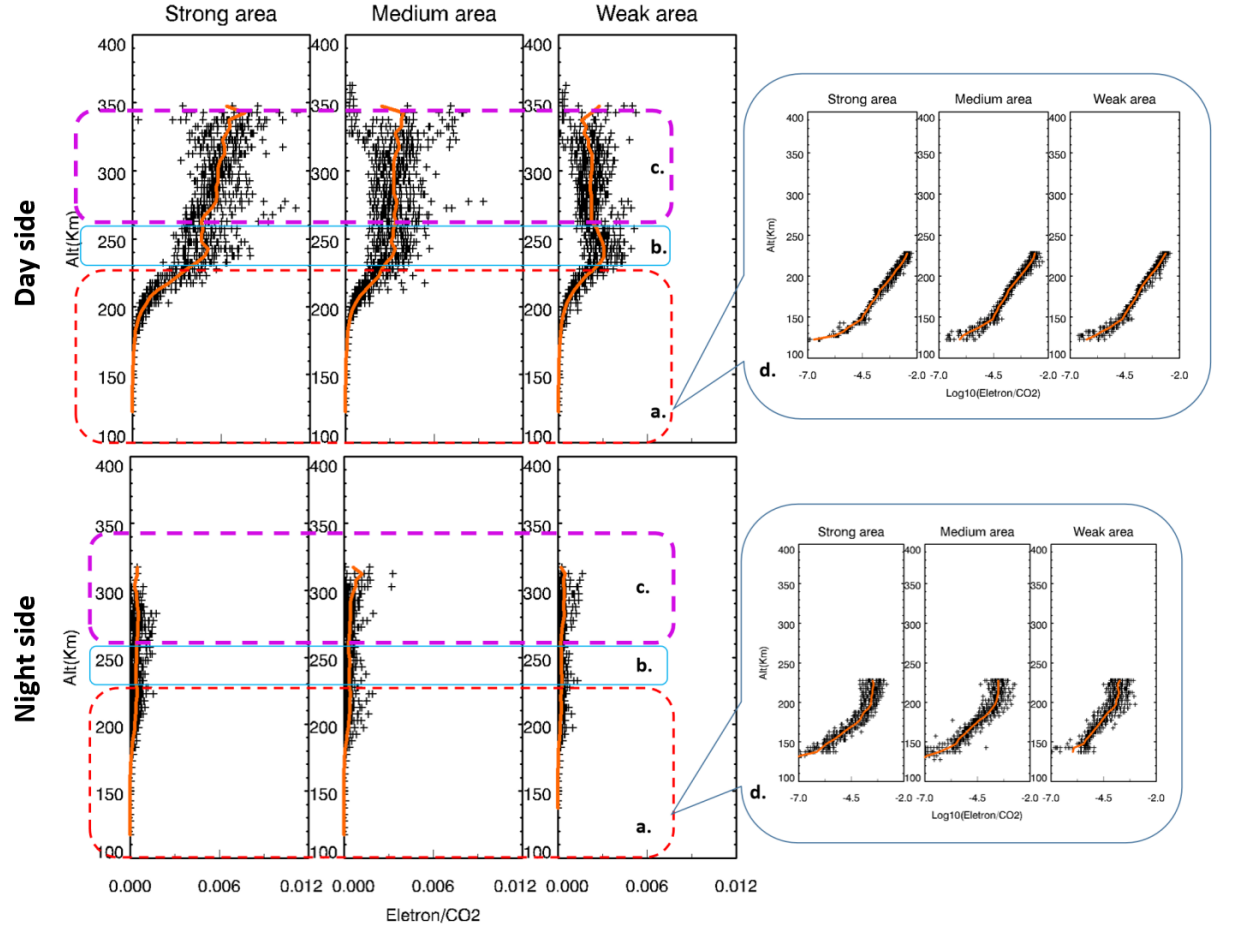


Figure 3. The ratio of N_e/N_{CO_2} (plus symbols) as a function of altitude in three categories of areas in both dayside and night-side. The plus symbols indicate the detected N_e/N_{CO_2} , and the orange bold line represent the averaged value of N_e/N_{CO_2} with an altitudinal resolution of 5 km. The right plane is logarithmic form of the ratio of N_e/N_{CO_2} below 230 km.

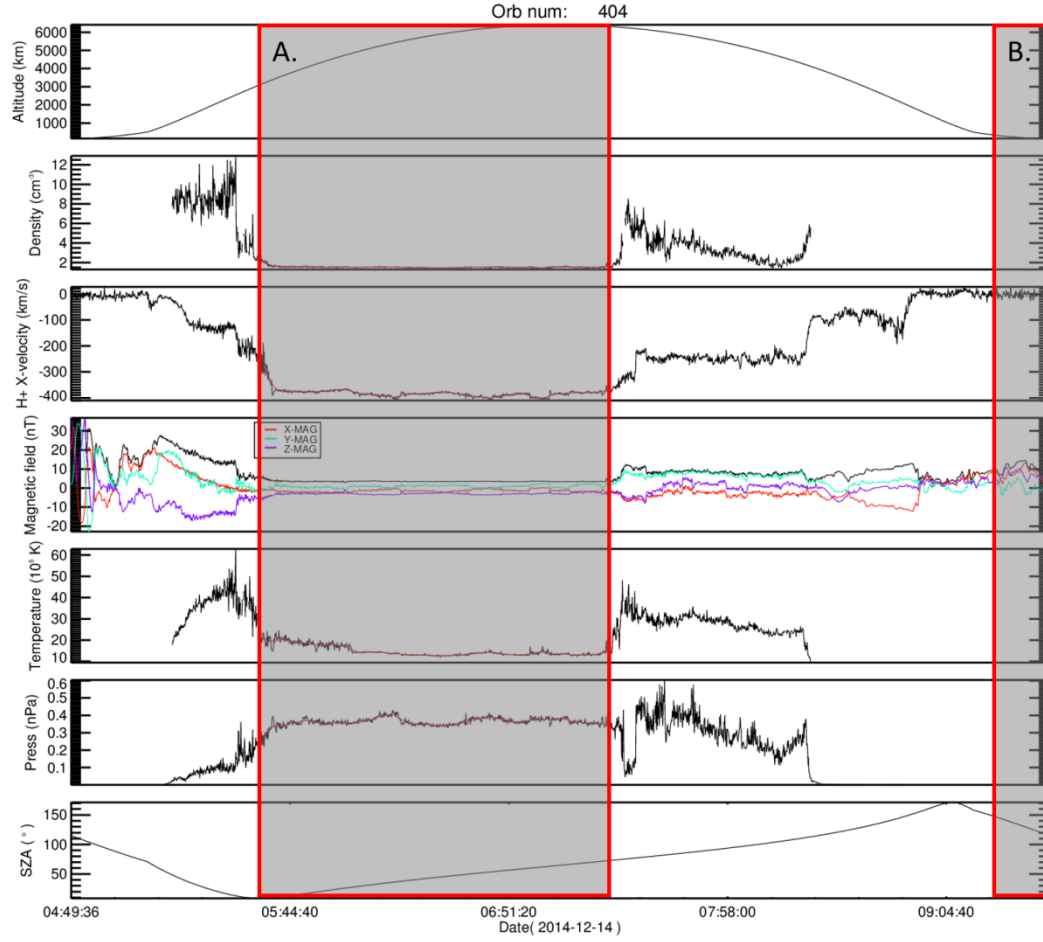


Figure 4. Plasmas and magnetic field parameters observed by MAVEN from 4:49:36 UT to 09:24:24 UT on 14 December 2014. From top to bottom: the local latitude of MAVEN spacecraft, electron density, H⁺ velocity X-component, magnetic field intensity (three components denoted by red, blue and purple lines, respectively), electron temperature, plasma pressure measured by MAVEN, solar zenith angle of MAVEN. The shaded part A denotes the area that MAVEN satellite operates in the solar wind. The shaded part B denote the MAVEN reenter ionosphere (the altitude is below 400 km).

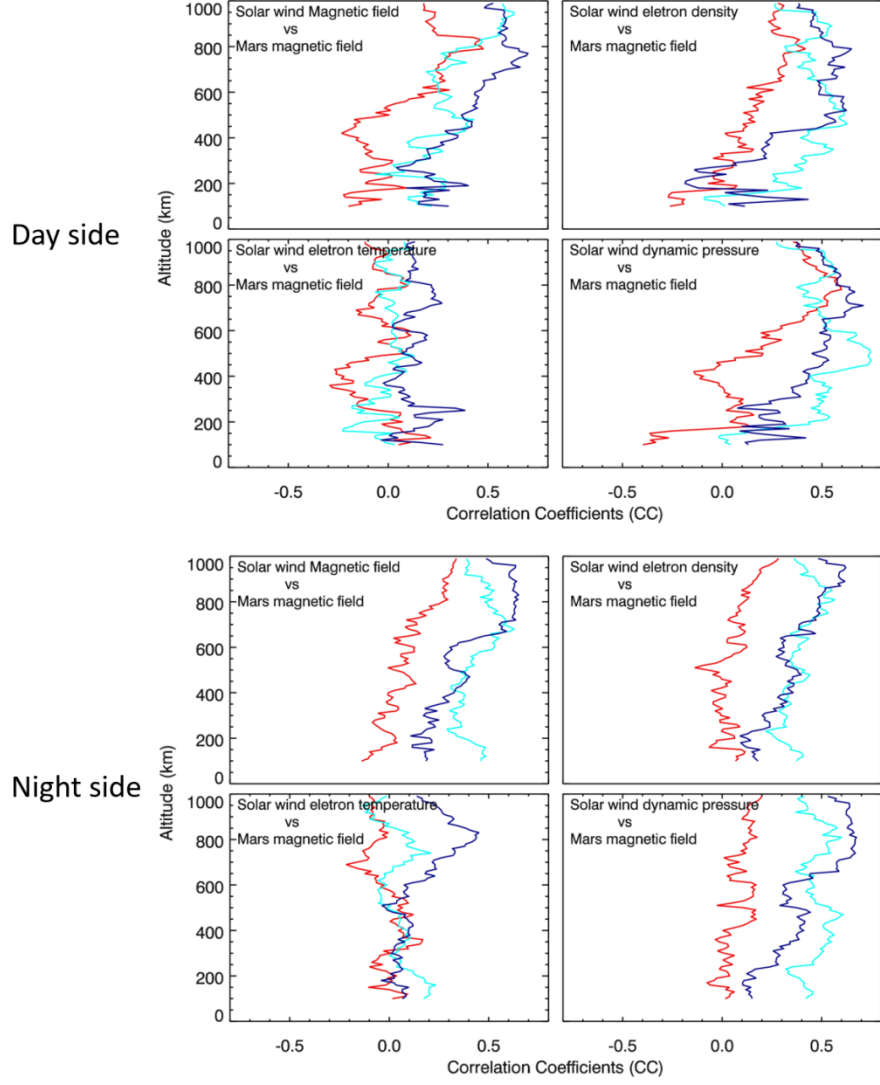


Figure 5. The CCs between Martian magnetic field and four solar wind parameters (including total magnetic field intensity, electron density, electron temperature and plasma pressure) as a function of altitude in the three categories of ionospheric magnetic field areas (the blue, cyan and red lines denote weak, median and strong areas, respectively). The top panels correspond to the CCs on dayside, and the bottom panels correspond to the CCs on nightside.

1. The intensity of magnetic field associated with solar wind

Since the intensity of Martian crustal magnetic field is very low, the topological structure of magnetic field is very vulnerable to external influence. In the below, the effects of solar wind on Martian ionospheric magnetic

field and the ratio of N_e/N_{CO_2} are analyzed. As MAVEN can cross from the ionosphere to solar wind, MAVEN can directly measure the parameters of solar wind around Mars. Here, an improved criterion, which is similar to the method of Marquette et al. (2018) and Halekas et al. (2017) is adopted to identify the region while MAVEN operate within the dayside solar wind.

1. $|V| > 200 \text{ km/s}$, where V is the proton speed.
 - 2) σ , where σ is a root-sum-squared value of the 32 Hz fluctuation levels in all three components of the IMF over a 4-s interval, is the IMF strength.
 - 3) T , where T is the proton scalar temperature.
1. the standard deviation of electron density is less than 0.15.
 2. zenith angle is less than 90° .

Through analysis of the database, we find that the regions in the solar wind can be validly identified using the criteria above. As an typical example shown in Figure 4, the characteristics of spcae environment from 05:44 UT to 07:25 UT on December 14, 2014 (as denoted by shaded part A) imply that the MAVEN operate in the solar wind during the time interval. On the other hand, after 09:14 UT (as denoted by shaded part B), when the altitude is less than 400 km, the MAVEN can be considered to enter Martian ionosphere. The averaged parameters of solar wind in part A are considered as the solar wind condition while the MAVEN reenter into the Martian ionosphere, although there is a time delay between them. Using the criterions above, a total number of 11040 orbits are selected to analyze the relationship between the ionospheric magnetic field (and the ratio of N_e/N_{CO_2}) and the solar wind. The correlation between four solar wind parameters and ionospheric magnetic field (including dayside and nightside) as a function of altitude in three categories of areas are calculated and shown in the Figure 5. It seems that the correlation between solar wind electron temperature and Martian ionospheric magnetic field are weak in all three categories of Martian magnetic field areas. On the other hand, the CC of ionospheric magnetic field and solar wind dynamic pressure is relatively high in weak and median magnetic field regions, especially for the median region, its CC is more than 0.5 at some altitudinal range, and the maximum value is more than 0.7.

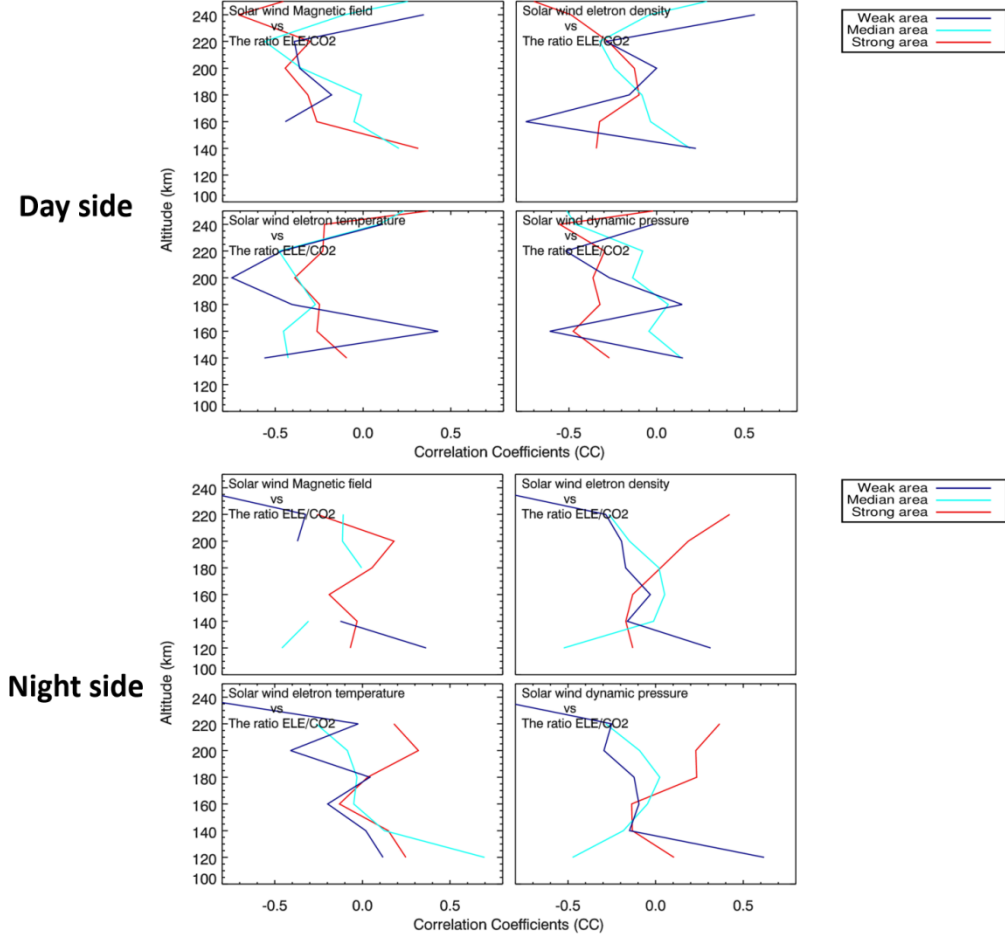


Figure 6. The CCs between the ratio of N_e/N_{CO_2} and four solar wind parameters (total magnetic field intensity, density, temperature and dynamic pressure) are calculated as a function of altitude in three categories of Martian magnetic field areas (the blue, cyan and red lines denote weak, median and strong areas, respectively). The top plane presents the CCs on dayside, and the bottom plane present the CCs on nightside.

The correlation between solar wind parameters and ionospheric ratio of N_e/N_{CO_2} as a function of altitude in the three categories of areas are calculated and exhibited in the Figure 6. Only the correlation below 260 km is exhibited, because the data above 260 km are inadequate. It seems that the correlation between solar wind electron temperature (electron density, and magnetic field) and ionospheric ratios of N_e/N_{CO_2} is little for both dayside and nightside. The correlation between solar wind dynamic pressure and nightside ionospheric ratio of N_e/N_{CO_2} is also weak. It reflects that the nightside ratio of N_e/N_{CO_2} is less affected by solar wind. However, there

is obvious negative correlation between solar wind dynamic pressure and dayside ionospheric ratio of N_e/N_{CO_2} in the region with strong ionospheric magnetic field. The correlation coefficient is around -0.45 above 150 km. This may imply that the dayside ionospheric plasmas are significantly escaped in response to enhanced solar wind dynamic pressure pulses in the dayside region with strong ionospheric magnetic field. On the other hand, there is weak correlation between solar wind dynamic pressure and dayside ionospheric ratios of N_e/N_{CO_2} in the both dayside regions with weak and median ionospheric magnetic field.

Discussion and Conclusions

In this paper, using the data measured by MAVEN, the ratio of N_e/N_{CO_2} in region with different levels of ionospheric magnetic fields are studied. We find that the variation of dayside ratio of N_e/N_{CO_2} ratio can be divided into three height ranges: below altitudinal 230 km, the presence of ionospheric magnetic fields have no effect on the dayside ratio of N_e/N_{CO_2} ; from altitudinal 230 km to 260 km, areas with strong ionospheric fields enhance the extremum value of dayside ratio of N_e/N_{CO_2} ; above altitudinal 260 km, the dayside ratio of N_e/N_{CO_2} obviously enhance with increase of altitude, and the ratio in stronger magnetic field area is larger. These results validate that the ratio of N_e/N_{CO_2} in region with strong ionospheric magnetic field is larger than other regions while the altitude is more than 230 km. This is similar with the results of previous works. For example, Flynn et al. (2017) reported that the presence of strong crustal fields has no effect on the electron density below 200 km altitude. Above 200 km altitude, electron density in areas with stronger magnetic fields is higher than that in surrounding regions. The high ratios of N_e/N_{CO_2} in regions of strong crustal fields could be explained by the fact that electrons in these regions are firmly trapped on closed field lines, because the most common field line topology was closed at altitudes between 200 and 400 km, and the field lines were even more likely to be closed in regions of strong ionospheric magnetic fields (Xu et al., 2017). The electrons can be trapped are more prevalent in strong ionospheric magnetic field regions than elsewhere (Flynn et al., 2017). On the other hand, in the regions with median and weak magnetic field, the magnetic field lines are significantly affected or produced by solar wind, thus forming dragged magnetic field line, they are often directly connected to the solar wind. As a result, the ratios of N_e/N_{CO_2} is very low in region with weak magnetic field.

Since the topological structure of magnetic field is very vulnerable to solar wind, in the study, we further explore the effect of solar wind on Martian ionospheric magnetic field and ionospheric magnetic field intensity. We find that the CCs between solar wind electron temperature (magnetic field intensity) and Martian ionospheric magnetic field are weak in all three categories of Martian magnetic field areas, but the CC of ionospheric magnetic field and solar wind dynamic pressure is relatively high, especially for the median region. This may imply

that the ionospheric plasma is significantly escaped in response to enhanced solar wind dynamic pressure in the dayside region with strong ionospheric magnetic field. It is similar to the conclusion in Ma et al., (2014), which suggest that the ionosphere responds almost instantaneously to the change in the solar wind dynamic pressure above 130 km. During extreme space weather events, the total escape of plasma fluxes could be about 2 orders of magnitude larger than those at quiet times (Ma and Nagy, 2007; Ma et al., 2014). In addition, there is weak correlation between solar wind dynamic pressure and dayside ionospheric ratio of N_e/N_{CO_2} in the both dayside regions with weak and median ionospheric magnetic field. It may be because that the magnetic field lines are significantly affected or produced by solar wind in these regions, thus forming dragged magnetic field line in these regions. The ionospheric magnetic field lines in these regions may be directly connect to the solar wind. During the interval of enhanced solar wind dynamic pressure, the plasma density of solar wind generally increases. As a result, the competition mechanism between increased solar wind density and obvious escaption bring about the low correlation. In addition, the correlation between solar wind dynamic pressure and ratio of night N_e/N_{CO_2} is weak for all three type regions, which means that the ratio of N_e/N_{CO_2} is less affected by solar wind.

The main conclusions are as follows:

1. The strong crustal field has no effect on the dayside ratio of N_e/N_{CO_2} below 260 km. While above 260 km, the ratio of dayside N_e/N_{CO_2} enhance with the increase of altitude, and the ratio of dayside N_e/N_{CO_2} is larger with stronger ionospheric magnetic fields.
2. The effect of crustal magnetic field intensity on the nightside ratio of N_e/N_{CO_2} is weak, the profiles of ratios in three classes of regions are similar.
3. The correlations of ionospheric magnetic field and solar wind dynamic pressure is relatively high, especially for the median region.
4. There is obvious negative correlation between dayside ratio of N_e/N_{CO_2} and solar wind dynamic pressure in the region with strong ionospheric magnetic field, which may imply that the ionospheric plasmas are significantly escaped in response to enhanced solar wind dynamic pressure pulses in the dayside region.
5. It seems that the effect of solar wind on nightside ratio of N_e/N_{CO_2} is very little.

Acknowledgments

The MAVEN data used in the present paper are from LASP (Laboratory for Atmosphere and Space Physics), University of Colorado, Boulder. We thank the organizations for making their data public. The effort at the Nanchang University was supported by the National Natural Science Foundation of China (grants 41974183, 42064009 and 41774195).

References

- Andersson, L., Ergun, R.E., Delory, G.T. et al (2015), The Langmuir Probe and Waves (LPW) Instrument for MAVEN. *Space Sci Rev* 195, 173–198, <https://doi.org/10.1007/s11214-015-0194-3>
- Andrews, D. J., N. J. T. Edberg, A. I. Eriksson, D. A. Gurnett, D. Morgan, F. Němec, and H. J. Opgenoorth (2015), Control of the topside Martian ionosphere by crustal magnetic fields. *J. Geophys. Res. Space Physics*, 120, 3042–3058, doi: 10.1002/2014JA0
- Barnes, J., Haberle, R., Wilson, R., Lewis, S., Murphy, J., & Read, P. (2017), The Global Circulation. In R. Haberle, R. Clancy, F. Forget, M. Smith, & R. Zurek (Eds.), *The Atmosphere and Climate of Mars* (Cambridge Planetary Science, pp. 229-294). Cambridge: Cambridge University Press. doi:10.1017/9781139060172.009
- Brain, Bagenal, Acuna, and Connerney (2003), Martian magnetic morphology: Contributions from the solar wind and crust, *J. Geophys. Res.*, 108, 1424, doi:10.1029/2002JA009482
- Connerney, Acuna, Wasilewski, Kletetschka, Ness, Reme, Lin, and Mitchell (2001), The global magnetic field of Mars and implications for crustal evolution, *Geophys. Res., Lett.*, 28, 4015-4018.
- Connerney, J. E. P., Espley, J., Lawton, P., Murphy, S., Odom, J., Oliverson, R. &
- Sheppard, D. (2015a), The MAVEN magnetic field investigation. *Space Sci. Rev.*, 195(1-4), 257-291, doi:10.1007/s11214-015-0169-4.
- Connerney, J. E. P., Espley, J., DiBraccio, G. A. et al. (2015b), first results of the magnetic field investigation. *Geophys. Res. Lett.*, 42(8819-8827, doi:10.1002/2015GL065366.
- Edberg, N. J. T., M. Lester, S. W. H. Cowley, and A. I. Eriksson (2008), Statistical analysis of the location of the Martian magnetic pileup boundary and bow shock and the influence of crustal magnetic fields, *J. Geophys. Res.*, 113, A08206, doi:10.1029/2008JA013096.
- Frahm, R.A., J.D. Winningham, J.R. Sharber, J.R. Scherrer (2006), Carbon dioxide photoelectron energy peaks at Mars., *Icarus*, 182 (2) 371–382.
- Flynn, C. L., Vogt, M. F., Withers, P., Andersson, L., England, S., & Liu, G. (2017), MAVEN observations of the effects of crustal magnetic fields on electron density and temperature in the Martian dayside ionosphere. *Geophysical Research: Letters*, 44, 10,812–10,821.
- Gurnett, D. A., R. L. Huff, D. D. Morgan, A. M. Persoon, T. F. Averkamp, D. L. Kirchner, F. Duru, F. Akalin, A. J. Kopf, E. Nielsen, A. Safaeinili, J. J. Plaut, and G. Picardi (2008), An overview of radar soundings of the Martian

ionosphere from the Mars Express spacecraft, *Adv. Space Res.*, 41, 1335-1346, doi:10.1016/j.asr.2007.01.062.

Halekas, J.S., Taylor, E.R., Dalton, G. et al. (2015), The Solar Wind Ion Analyzer for MAVEN. *Space Sci Rev* 195, 125–151, <https://doi.org/10.1007/s11214-013-0029-z>

Halekas J S, Ruhunusiri S, Harada Y, et al. (2017), Structure, dynamics and seasonal variability of the Mars-solar wind interaction: MAVEN Solar Wind Ion Analyzer in-flight performance and science results[J]. *Journal of Geophysical Research: Space Physics*, 122: 547-578.

Halekas, J. S., Ruhunusiri, S., Harada, Y., Collinson, G., Mitchell, D. L., Mazelle, C., et al. (2017), Structure, dynamics, and seasonal variability of the Mars-solar wind interaction: MAVEN Solar Wind Ion Analyzer in-flight performance and science results. *Journal of Geophysical Research: Space Physics*, 122, 547–578. <https://doi.org/10.1002/2016JA023167>

Hara, T., Luhmann, J. G., Leblanc, F., Curry, S. M., Halekas, J. S., Seki, K., et al. (2018), Evidence for crustal magnetic field control of ions precipitating into the upper atmosphere of Mars. *Journal of Geophysical Research: Space Physics*, 123, 8572–8586.

Ma, Y.-J., and A. F. Nagy (2007), Ion escape fluxes from Mars, *Geophys. Res. Lett.*, 34, L08201, doi:10.1029/2006GL029208.

Ma, Y. J., X. Fang, A. F. Nagy, C. T. Russell, and G. Toth (2014), Martian ionospheric responses to dynamic pressure enhancements in the solar wind, *Journal of Geophysical Research: Space Physics*, 119 (2), 1272–1286, doi:10.1002/2013JA019402, 2013JA019402.

Mahaffy, P.R., Benna, M., King, T. et al. (2015), The Neutral Gas and Ion Mass Spectrometer on the Mars Atmosphere and Volatile Evolution Mission. *Space Sci Rev* 195, 49–73. <https://doi.org/10.1007/s11214-014-0091-1>

Marquette, M., Lillis, R. J., Halekas, J. S., Luhmann, J. G., Gruesbeck, J. R., & Espley, J. R. (2018), Autocorrelation study of solar wind plasma and IMF properties as measured by the MAVEN spacecraft. *Journal of Geophysical Research: Space Physics*, 123, 2493–2512. <https://doi.org/10.1002/2018JA025209>

Sakai, S., Seki, K., Terada, N., Shinagawa, H., Tanaka, T., & Ebihara, Y. (2018), Effects of a weak intrinsic magnetic field on atmospheric escape from Mars. *Geophysical Research Letters*, 45, 9336–9343.

Withers, P., M. J. Mendillo, H. Rishbeth, D. P. Hinson, and J. Arkani-Hamed (2005), Ionospheric characteristics above Martian crustal magnetic anomalies, *Geophys. Res. Lett.*, 32, L16204, doi:10.1029/2005GL023483.

Withers, P. (2009), A review of observed variability in the dayside ionosphere of Mars, *Adv. in Space Res.*, 44, 277-307, doi:10.1016/j.asr.2009.04.027

Xu, S., et al. (2017), Martian low-altitude magnetic topology deduced from MAVEN/SWEA observations, *J. Geophys. Res. Space Physics*, 122, 1831–1852, doi:10.1002/2016JA023467.